

**Control of the magnetism of cobalt phthalocyanine by a ferromagnetic substrate**Emilia Annese,<sup>1,2,\*</sup> Jun Fujii,<sup>1</sup> Ivana Vobornik,<sup>1</sup> Giancarlo Panaccione,<sup>1</sup> and Giorgio Rossi<sup>1,2</sup><sup>1</sup>TASC Laboratory, IOM-CNR, SS 14, km 163.5, I-34149 Trieste, Italy<sup>2</sup>Dipartimento di Fisica, Università di Modena e Reggio Emilia, via Campi 213/A, I-41100 Modena, Italy

(Received 4 May 2011; revised manuscript received 30 September 2011; published 30 November 2011)

The electronic and magnetic properties of cobalt-phthalocyanine (CoPc) molecules are modified at the interface with a magnetic metallic surface: upon adsorption of CoPc on iron film relevant changes are observed in the C 1s photoemission line shape and on Co  $L_{2,3}$  edges, and N  $K$ -edge x-ray absorption spectra. X-ray magnetic circular dichroism shows Co  $3d$  spin-polarized states, i.e., magnetic coupling with the iron substrate at room temperature. The interplay among the electronic and magnetic properties and CoPc adsorption sites is fundamental for tailoring the functionalities of hybrid organic-metallic interfaces.

DOI: [10.1103/PhysRevB.84.174443](https://doi.org/10.1103/PhysRevB.84.174443)

PACS number(s): 75.50.Xx, 73.20.Hb, 79.60.Dp, 85.75.-d

**I. INTRODUCTION**

One goal of spintronics is to achieve control of spin alignment in matter by electrical manipulation.<sup>1</sup> Organic spin valves operating at low temperature show magnetoresistance response when applying a bias of a few millivolts.<sup>2</sup> The magnetic coupling between organic films and magnetic substrate in hybrid interfaces can play an important role in stabilizing the electronic states. The understanding of the onset of magnetism in the molecular organic film at room temperature represents one of the challenging issues in both the fundamentals of spin physics at interfaces and in understanding possible spintronics functionalities. Paramagnetic molecules in fact represent a promising option in spin manipulation with the aim of minimizing the single magnetic unit.<sup>3-6</sup> These systems have the advantage to be more flexible and robust with respect to single adatoms<sup>7</sup> and their weak spin-orbit interaction should favor the establishment of spin current over a distance in the order of tens of nanometers.<sup>8-10</sup>

The magnetic properties of different organic molecules adsorbed on magnetic and nonmagnetic metal was recently characterized.<sup>4-7</sup> For instance, the magnetic anisotropy of a two-dimensional supramolecular network of organic molecules on Cu(100) was controlled by the adsorption of oxygen. In these cases the alignment of the central atom's spin occurs in a high applied magnetic field (6 T) and a very low temperature (8 K).<sup>6,11-13</sup> On the other hand, when ferromagnetic materials are used as substrates, the coupling of the organic molecules and magnetic substrate appears even at room temperature.<sup>14-17</sup> In iron-porphyrin the magnetic moment of the host atom can be rotated along the direction in plane as well as out of plane by a magnetization reversal of the substrate.<sup>15,16</sup> In many of these studies the coupling at the organic-inorganic interface is driven by the direct exchange interaction between the magnetic substrate and the central metal of molecules.<sup>15,16</sup> In other cases the magnetic coupling between the organic molecule and the magnetic substrate occurs through N molecular sites.<sup>18</sup>

Among paramagnetic molecules, porphyrin (P) and phthalocyanines (Pc) are used in chemical sensors, optoelectronic devices, prototypes of solar cells, and field-effect transistors.<sup>19</sup> Both types of molecules are quasiplanar heterocyclic macrocycles with high conjugation. They present different end groups

that lead to different functionalization. Both molecules are able to coordinate metal cations in their centers by binding with the four central nitrogen atoms, producing metal-porphyrin (M-P) and metal-phthalocyanine (M-Pc). What makes these metal-organic molecules unique is the possibility to tune their structural, chemical, magnetic, and transport properties by means of changing different cations within the macrocycle or by changing ligands. The configuration of the ground states of a transition-metal atom placed in the center of the macrocycle depends on the ligand field splitting, to which corresponds a big variety of different electronic and magnetic ground states. For instance, the magnetic properties of CoPc arise from unpaired spins in the  $3d$  orbitals of the central atom. CoPc has a magnetic moment of  $1.09\mu_B$  (Ref. 20) (much smaller than the isolated  $\text{Co}^{2+}$  ion, i.e.,  $5\mu_B$ ), but, as a free molecule, it is paramagnetic. The interaction with the magnetic substrate offers the interesting possibility of orienting and controlling the CoPc moment. The magnetic coupling occurs when spins of individual molecules undergo ordering due to the interaction with the substrate.

Different scenarios have been observed in the case of the CoPc molecule: the central atom loses its magnetic moment upon adsorption on gold substrate,<sup>21,22</sup> the Co molecular magnetic moment is reduced upon adsorption on the Co magnetically oriented nanoisland, but manifests an exchange interaction with the substrate;<sup>23</sup> the Co molecular magnetic moment is quenched upon adsorption on Fe ferromagnetic film, but spin-polarized scanning-tunneling microscopy (STM) images showed the magnetic spin polarization resolved on a submolecular scale.<sup>24</sup> According to these studies the magnetic response of the molecule was found to depend on the adsorption site and electronic density of state of the molecule modified upon adsorption.

Our study provides further understanding of the interplay among the electronic, the magnetic interaction, and the adsorption geometry of CoPc on the ferromagnetic substrate at room temperature. We have chosen iron film grown on Cu(111) as a magnetic substrate. Fe magnetization switches from perpendicular [thickness  $<5$  monolayer (ML)] to parallel to the surface (thickness  $>10$  ML).<sup>25</sup> This substrate permits one to explore the coupling of the magnetic moment of the molecule along the easy magnetization direction, depending on the thickness of the iron film. The local arrangement

and orientation of the molecules was established by STM and by angle-dependent x-ray absorption spectroscopy (XAS) exploiting the search light effect with linearly polarized soft x rays.<sup>26</sup> CoPc molecules adsorb with their molecular plane parallel to the iron film. The formation of bonding between the molecule and Fe induces a strong modification of the electronic properties of the molecule at the N and C sites. We observed evidence of a direct magnetic coupling between the Co atoms in the molecule and the iron film.

## II. EXPERIMENT DETAILS

Sample preparation and characterizations have been performed at APE beamline of IOM-CNR at the Elettra synchrotron radiation facility (Trieste). The photon beam provided by Apple II undulators can be chosen both linearly and circularly polarized.<sup>28</sup> XAS measurements were performed measuring the sample drain current with an energy resolution of 150 meV. X-ray magnetic circular dichroism (XMCD) spectra were recorded with a fixed helicity of the light and at remanence, i.e., reversing the magnetization direction for each point of the spectra. X-ray photoemission spectra (XPS) data have been acquired by a seven channel Omicron EA-125 analyzer at normal emission using linearly polarized x rays with photon energies of 480 eV. The overall energy resolution (photons + analyzer) was about 200 meV. All preparation and characterization chambers are connected in UHV.<sup>28</sup> STM images were acquired in UHV on the same samples with atomic resolution. STM measurements were recorded at RT. STM data analysis and representation is made using WSXM software.<sup>29</sup>

The Cu(111) substrate is prepared *in situ* by several cycles of Ar<sup>+</sup> sputtering and annealing. Iron is deposited on the substrate by electron beam evaporator in a base pressure of  $\sim 10^{-10}$  mbar. CoPc is evaporated *in situ* by molecular beam deposition from a resistively heated quartz crucible in a base pressure of  $\sim 10^{-10}$  mbar. The thickness is estimated by quartz microbalance.

## III. RESULTS AND DISCUSSIONS

The orientation of the molecules depends on substrate roughness, molecule/substrate and molecule/molecule interactions. A high degree of ordering for phthalocyanines was observed in many thin films; generally, molecules stand on rough substrates and lie flat on the single-crystalline metallic substrates.<sup>30,31</sup> We have determined the geometry and orientation of the molecules by means of STM and angle-dependent XAS at the N K edge.

In Fig. 1 we show STM analysis of the three stages of sample preparation: the clean Cu(111) surface (a), the iron epitaxial film (b), and the CoPc ML on the iron film (c). Figure 1(b) displays the morphology of the iron 20-ML-thick film after deposition and thermal treatment: the substrate is uniformly covered by three-dimensional Fe clusters of lateral dimension  $16 \times 20 \text{ nm}^2$  (in average) corresponding to Fe(110) bcc islands. The molecules adsorb flat with their macrocycle parallel to the Fe island surface and organize in two local lattices: rectangular with lattice parameters  $1.6 \times 1.6 \text{ nm}^2$  and hexagonal lattice with a molecule-molecule distance of

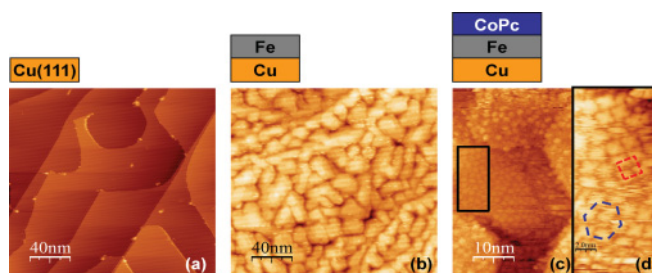


FIG. 1. (Color online) The quality of the Cu(111) surface (a) and the growth of iron film (b) were monitored by STM. CoPc molecules adsorb flat on the Fe/Cu(111) surface as shown in the STM images [(c),(d)]. Bias and tunneling current of the images: (a)  $V_b = -1 \text{ V}$ ,  $I = 0.08 \text{ nA}$ ; (b)  $V_b = -0.8 \text{ V}$ ,  $I = 0.6 \text{ nA}$ ; (c)  $V_b = -0.6 \text{ V}$ ,  $I = 0.32 \text{ nA}$ .

$\sim 1.53 \text{ nm}$  [Figs. 1(c) and 1(d)]. CoPc molecules are identified by the four-lobed pattern (related to the charge in the four aromatic rings of the Pc structure).

STM results indicate that CoPc lies flat onto the substrate which is a signature of a stronger phthalocyanine-iron interaction with respect to the intermolecular interaction. The lying down adsorption of CoPc on iron is in agreement with reports on similar molecule/metal interfaces.<sup>30,31</sup>

Figure 2(a) shows the N 1s XAS spectrum for 1 and 6 ML CoPc on the iron film and 1 ML CoPc on the pristine Cu(111) surface ( $\theta = 60^\circ$ ). N 1s XAS spectra of molecular films are characterized by two different energy regions: the first with well-resolved peaks below 403.6 eV relative to the  $1s-\pi^*$  transitions (i.e., transitions into the lowest unoccupied molecular orbital, LUMO, and the next unoccupied states: LUMO+1 and LUMO+2); the second with broad features at higher photon energies are due to  $1s-\sigma^*$  transitions. The N 1s XAS spectrum for the 6 ML CoPc film shows representative features due to the contribution of two different N sites [N<sub>1</sub> and N<sub>2</sub> as defined in the CoPc sketch reported in Fig. 3(a)]. The CoPc layer, in direct contact with iron film, shows broadened features in the  $\pi^*$  region well distinguished from the multilayer spectrum. The change in the spectral line shape indicates that the electronic properties of CoPc on the N site are different at or away from the CoPc/Fe interface. This behavior is characteristic for the CoPc/Fe interface; in fact, the N 1s XAS spectrum of the CoPc/Cu(111) interface [Fig. 2(a)] displays

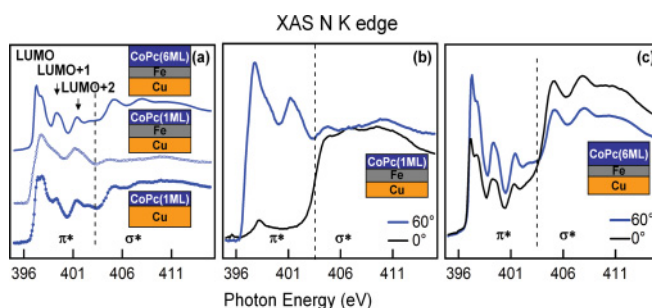


FIG. 2. (Color online) (a) N 1s XAS spectra ( $\theta = 60^\circ$ ) of 1 ML (hollow circle) and 6 ML (line) CoPc on Fe film and 1 ML CoPc (circle) on Cu(111). Angle-dependent N K XAS spectra shown for 1 ML (b) and 6 ML (c) of CoPc film on Fe. The measurements were performed at room temperature.

a similar line shape to the CoPc multilayer spectra, except for a reduction of the LUMO intensity. To further understand this effect, we underline the differences among the CoPc multilayer and the CoPc/Fe and CoPc/Cu interfaces. The spectrum of the CoPc multilayer is the closest approximation to that of the free-like molecule, being the molecule-molecule interaction is rather weak. CoPc preferentially adsorbs in the bridge position on the Cu(111) substrate.<sup>32</sup> Electronic charge redistribution occurs at the CoPc/Cu interface with a reduction of LUMO at both N and Co sites, compatible with a charge transfer from the substrate to the molecule.<sup>20,33</sup> On the other hand, CoPc adsorbs in the top position on thin iron film, with Co at the vertical of the substrate atom according to Ref. 24. In panel (b) of Fig. 3, a sketch of a possible top site for the molecule on Fe(110) film is reported.<sup>34</sup> In this geometry, N<sub>1</sub> atoms are affected by the presence of iron atoms inducing a strong modification of N electronic structure at the CoPc/Fe interface. The onset of a direct bonding between the N atoms and the iron film can be at the origin of the N 1s spectral line shape similarly to MnPc adsorbed on Co.<sup>17</sup> Another explanation for the spectral broadening of the N 1s spectrum relative to the CoPc/Fe interface is that the charge transfer between Fe and N is much larger compared to that between Cu and N, possibly due to the different density of state for Fe and Cu near the Fermi level. Charge redistribution at the interface is reflected in the complex structure of the spectra that cannot directly reveal the amount and sign of net charge transfer.

In addition to the spectral line shape analysis, more information can be inferred by the angle-dependent XAS spectra measured at the N K edge. In planar  $\pi$ -conjugated systems  $\pi^*$  orbitals are expected to be out of molecular plane, while  $\sigma^*$  are oriented in the molecular plane. Figure 2(b) displays the N K-edge XAS performed for the CoPc(1 ML)/Fe interface at normal ( $0^\circ$ ) and grazing ( $60^\circ$ ) incidence, with polarization vector  $\mathbf{E}$  parallel and perpendicular to the molecule plane [experimental geometry: Fig. 3]. The disappearance of the  $\pi^*$  resonances (except for a residual intensity at about 496.8 eV) when  $\mathbf{E}$  is in the molecular plane demonstrates that N atoms lay in a plane parallel to the substrate, consistently with the STM real-space images. On the other hand, the spectra of the CoPc multilayer in Fig. 2(c) show only a weak angular dependence of the first pair of  $\pi^*$  resonances. The difference in N 1s  $\rightarrow \pi^*$  XAS intensity

behavior for the CoPc multilayer and monolayer at grazing incidence indicates the superposition of different molecular orientations that can be laterally or perpendicularly distributed.

We exploit the chemical sensitivity of x-ray photoemission and x-ray absorption to probe the electronic properties at different molecular sites for each molecule/substrate interface. The change in the chemical bonding of the element corresponds to the change in binding energy in the core electron photoemission. The response of a highly polarized  $\pi$ -electron framework to a localized core hole created in an adjacent molecule can lead to satellite features or shake-up states, whose energies and intensities reflect specific channels for intermolecular coupling or substrate/molecule interaction.

In Figs. 4(a) and 4(b) C 1s and N 1s core-level spectra of 1 and 6 ML CoPc on iron film and 1 ML CoPc on Cu(111) (bottom spectra) are reported. The C 1s core-level photoemission spectrum of 6 ML CoPc reflects two different C sites (C within the benzene ring, C<sub>b</sub>, and C within the pyrrole, C<sub>p</sub>) and satellites originated by the shake-up (S)  $\pi^*-\pi^*$  process [the expected transition occurs at  $\sim 1.8$  eV (Ref. 35)] and a further feature at a low binding energy with respect to the main peak. The low binding-energy feature originates from residual C impurity on the iron film and can be removed by subtracting the spectrum of pristine iron (blue line aligned with C 1s spectrum). To describe the C 1s XPS spectrum we used a fitting function as shown in Fig. 4(a). The relevant parameters of the fit are the C<sub>b</sub>-C<sub>p</sub> peak relative energy shift, their relative intensities, and shake-up satellite intensity.<sup>36-38</sup> The interaction with Fe substrate leads to a binding-energy shift of C features of about 0.2 eV to a lower binding energy and to a reduction of C<sub>b</sub>-C<sub>p</sub> energy separation [from 1.38 (0.08) eV in 6 ML CoPc to 1.01 (0.08) eV in ML CoPc]. We also observed a reduced intensity ratio of benzene/pyrrole features with respect to 3:1 as expected for the free molecule. The change in the relative intensities indicates that benzene carbon atoms are more directly affected by the interaction with the substrate. For the CoPc/Fe interface, C 1s ionization produces satellite features which are nearly constant in energy, but with enhanced intensity (vertical dashed region). The increase in the intensity of shake-up satellites in the C 1s XPS spectrum is interpreted as a bigger intermolecular charge transfer mediated by the substrate.<sup>39</sup> This produces an overall change in the C 1s line shape with the onset of an asymmetric tail similar to the many-body excitation spectrum of the metallic core level. The asymmetric tail is characteristic for CoPc/Fe and is absent in the CoPc/Cu(111) interface [see the bottom spectrum in Fig. 4(a)], where to the contrary a reduction in the shake-up intensity is compatible with a charge transfer from the substrate to the molecule.<sup>33</sup>

The two N sites of CoPc have binding energies that are not resolved in the photoemission spectra. The N 1s core-level spectrum of the CoPc multilayer [Fig. 3(b), top spectrum] consists of a main feature and a faint high binding-energy contribution ( $\sim 401$  eV) attributed to shake-up satellites. Due to the interaction with Fe substrate the N 1s feature [Fig. 2(b), bottom spectrum] undergoes a shift of 0.3 (1) eV to a lower binding energy and the line shape displays a further component at a lower binding energy (398.5 eV).

The 3d band of the host central atom, Co, is split because of the ligand field. In the case of the free-like CoPc molecule Co is divalent ( $3d^7$ ) and the ligand field has  $D_{4h}$  symmetry, with

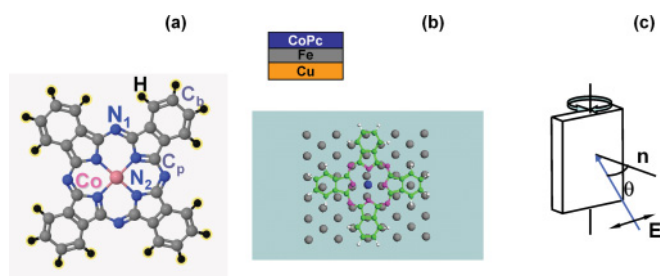


FIG. 3. (Color online) (a) CoPc structure; (b) CoPc adsorption on top Fe site (Ref. 21); and (c) the geometry of the N K XAS experiment: the orientation of the electric field vector  $\mathbf{E}$  varies from parallel (normal incidence:  $\theta = 0^\circ$ ) to upright (grazing incidence:  $\theta = 60^\circ$ ) to the sample surface depending on the incidence angle of the synchrotron light.

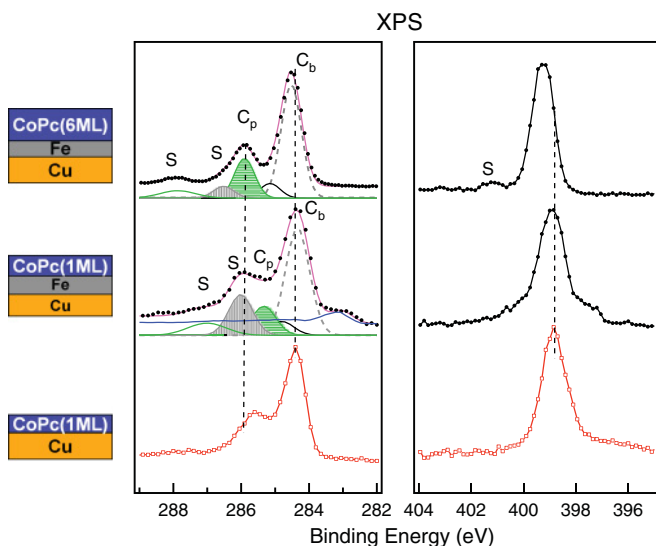


FIG. 4. (Color online) (a) C  $1s$  and (b) N  $1s$  core-level photoemission spectra of 1 ML and 6 ML CoPc film on iron measured with a photon energy of 480 eV. The C  $1s$  and N  $1s$  core-level photoemission spectra relative to 1 ML of CoPc on Cu(111) are reported at the bottom of panels (a) and (b). The photoemission spectra are aligned with respect to the Fermi edge. The intensity of the spectra is normalized to a peak height of the most intense component to highlight changes in the line shape. (a) C  $1s$  XPS: Data (dots) and peaks fit (solid line) are shown for 1 ML (middle) and 6 ML (top) CoPc film on iron. Five components with gaussian profile are used in the curve fitting for C  $1s$  spectra (dots) with a FWHM of circa 0.5 eV. They accounts for two different C sites:  $C_b$  [dashed line (green dashed line)] and  $C_p$  [horizontal line pattern (green horizontal line pattern)] within CoPc and their shake-up satellites relative to  $C_b$  [vertical line pattern (gray vertical line pattern)] and  $C_p$  [gray line (green line)] respectively and a vibrational feature (black line) close to  $C_b$ . The feature at low binding energy is subtracted from C  $1s$  XPS spectra of pristine iron film (blue line aligned with C  $1s$  spectrum).

possible low or high spin configuration. Many experimental and theoretical investigations predict a completely empty  $3d_{x^2-y^2}$  orbital, but different half-filled orbitals: either  $3d_{xy}$ ,  $3d_{xz,yz}$ , or  $3d_{3z^2-r^2}$ . The possible electronic configurations of CoPc ground states were reduced to two, discernible as a function of temperature, but equally describing room temperature Co  $L_{2,3}$  XAS spectra of the CoPc multilayer.<sup>41</sup> Recently, XAS and XMCD experimental results and simulations at low temperature provided the CoPc electronic structure without ambiguity. Spin-orbit coupling mixes CoPc ground and excited states, with a configuration  $(e_g)^{3.8}(b_{2g})^2(a_{1g})^{1.2}$ , inducing finite in-plane orbital moment in the ground state.<sup>22,41</sup>

Co  $L_{2,3}$  XAS spectra probe the unoccupied  $s$  and  $d$  states of the molecule as projected to the Co site. The spin-orbit coupling of the  $2p$  core hole of the excited state with  $j = 3/2$  ( $L_3$ ) and  $j = 1/2$  ( $L_2$ ) appears in the XAS spectra as two main peaks separated by  $\sim 15$  eV. Figures 5(a) and 5(b) report Co  $L_{2,3}$  XAS spectra at selected incident angles,  $\theta$ , for the CoPc multilayer ( $T = 80$  K) and monolayer ( $T = 300$  K), respectively.

Co XAS is superimposed to a nonlinear background originating from ejecting photoelectrons after excitation at Fe edges and interacting in the surroundings of nonexcited

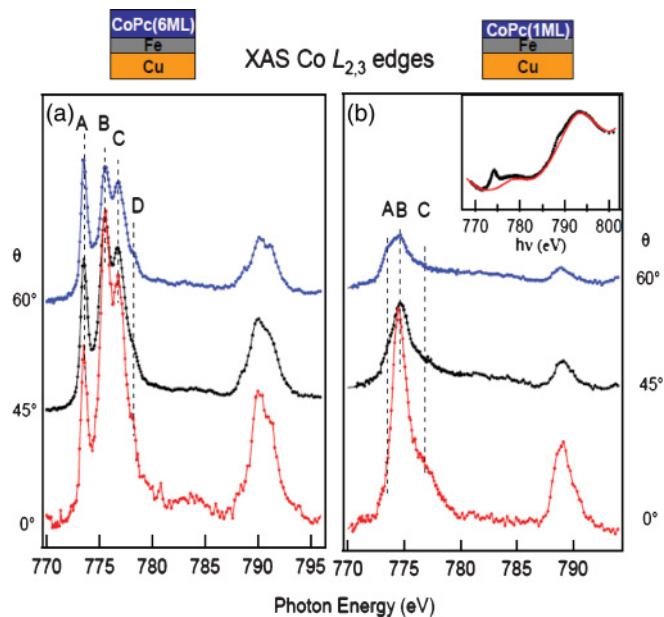


FIG. 5. (Color online) Co  $L_{2,3}$  XAS spectra are shown for CoPc films: 6 ML (a) and 1 ML (b) grown on Fe(20 ML)/Cu(111) after Fe background subtraction. The spectra were taken at different incident angles  $\theta$  between the polarization vector  $\mathbf{E}$  and the normal to the sample surface. Co  $L_{2,3}$  XAS spectra of 6 ML CoPc film on iron were acquired at 80 K. All spectra were normalized to 1 at the high-energy side. The same color code was used to denote the spectra measured at the same incident angles ( $0^\circ$ , red;  $45^\circ$ , black;  $60^\circ$ , blue) in both panels. The inset in (b) reports the row XAS data at the Co  $L_{2,3}$  edges for 1 ML CoPc (circle) and iron film (line).

atoms [iron extended x-ray fine structure (EXAFS)]. Iron contribution in the spectra is more evident in 1 ML CoPc, where the amount of Co is 3% of the Fe atoms. Evidence of Fe contribution is also in the XAS measurements on the CoPc multilayer, but less intense. In the inset of Fig. 5(b) the Co XAS data as measured for 1 ML CoPc on Fe (circle) and for the Fe surface (line) are reported. We subtracted from the spectrum of 1 ML CoPc on Fe that of the pristine iron film to remove the iron contribution to Co  $L_{2,3}$  XAS. All the measurements reported in Fig. 5 are obtained with the data treatment explained above.

The spectrum relative to the multilayer shows several spectral features: 773.5 (A), 775.7 (B), 777 (C), and 778.2 eV (D) consistent with the  $\text{Co}^{2+}$  valence state. Co  $L_3$  XAS spectral intensities vary as a function of the incident angle and reveal the spatial distribution of unoccupied  $3d$  orbitals, which are expected to be out or within the molecular plane. In the CoPc multilayer, the intensity of feature A increases with the incident angle, whereas the opposite occurs for the remaining features (B, C, and D). The linear dichroism of feature A demonstrates that the corresponding  $3d$  orbital lies out of the molecular plane. Moreover, the line shape of the spectrum with a large projection of  $\mathbf{E}$  on the normal to the surface ( $60^\circ$ ) is similar to the CoPc multilayer on gold measured at room temperature.<sup>40</sup> Our results are compatible with the electronic configuration proposed for CoPc in Refs. 22 and 40.

The XAS spectral shape changes drastically for the CoPc/Fe interface, as shown in Fig. 5(b). The peak *D* on the high-energy side of the  $L_3$  edge has vanished, whereas feature *A* is very much reduced with respect to the multilayer. The Co  $L_3$  XAS spectra of the CoPc/Fe interface display intensity evolution as a function of angle similar to that of 6 ML CoPc, i.e., the spectral intensity relative to the out-of-plane molecular component (*A*) of the  $3d$  orbital increases with angle, whereas it decreases for  $3d$  orbitals (*B,C*) in the plane of the molecule. Co XAS spectra relative to the CoPc/Fe interface indicates that  $3d$  orbitals are mainly oriented in plane. Similarly to the CoPc/Au(111) interface the  $3d$  electronic ground state of CoPc is modified with respect to that of the multilayer and possibly can be expressed as a superposition of the Co  $d^7$  and  $d^8$  configurations.<sup>22</sup>

The change in Co  $3d$  electronic distribution directly influences the Co magnetic moment and therefore the magnetic coupling with the substrate. Calculations predict a reduction of the Co magnetic moment upon adsorption at Co(111) by one-third<sup>20</sup> and a null magnetic moment at the CoPc/Fe(110) interface.<sup>24</sup>

We have measured XMCD spectra with circularly polarized soft x rays at the  $L_{2,3}$  characteristic edges of Fe and Co in order to detect independently the magnetic order of the molecular film and substrate. XMCD exploits the differential absorption when the alignment between magnetization and photon helicity switches from parallel to antiparallel. The XMCD signal reflects the spin and orbital moments of the molecular central atom.<sup>27</sup>

For 20 ML Fe/Cu(111) the easy axis of magnetization is pointing parallel to the surface, i.e., parallel to the molecular plane of CoPc. XAS spectra recorded at Fe  $L_{2,3}$  with circularly polarized light with photon helicity parallel and antiparallel to the magnetization are reported in Fig. 6(a) and are indicated as  $I^+$  and  $I^-$ , respectively. The XMCD spectrum at the  $L_{2,3}$  edges of Fe confirms the alignment of Fe spins along the surface magnetization vector. The Fe XMCD asymmetry defined as  $[I^+ - I^-]/[I^+ + I^-]$  is 18%. The field-dependent Fe  $L_3$  XMCD intensity is reported at a fixed photon energy and describes the Fe square hysteresis loop at room temperature with a coercive field of 50 (0.5) Oersted.

In Fig. 6(c) we report Co XAS coefficients  $I^+$  and  $I^-$ , which are the difference spectra obtained by subtracting the spectrum relative to the Fe surface to that of 1 ML CoPc. The difference between row Co XAS spectra for parallel and antiparallel orientation of the magnetization and the light polarization does not give the Co XMCD signal, because the superimposed iron EXAFS oscillations are also dichroic (the EXAFS dichroic signal is one order of magnitude smaller than that of the XAS Fe  $L_{2,3}$  edges<sup>42</sup>). Therefore, the Co XMCD spectrum is obtained by subtracting difference spectra  $I^-$  from  $I^+$ . The estimated error related to this data analysis is 50% of the measured Co XMCD signal.

The XMCD spectrum shows dichroism both at the  $L_3$  and  $L_2$  edges, with the same sign displayed by the iron film. This indicates that CoPc is ferromagnetically coupled with the iron film. The Co XMCD asymmetry is  $3.6(\pm 1.8)\%$ .

The presence of XMCD in 1 ML CoPc on iron film implies that modeling the CoPc adsorption on iron with the full transfer of the  $d_{z^2}$  electron and consequent loss of local

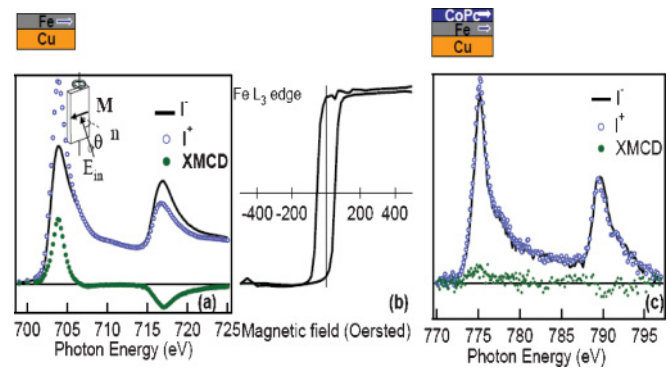


FIG. 6. (Color online) Fe  $L_{2,3}$  XAS spectra relative to the parallel  $I^+$  (dots) and antiparallel  $I^-$  (line) orientations of magnetization and light polarization and XMCD ( $I^+ - I^-$ ) spectra of iron film grown on Cu(111). The scheme in panel (a) illustrates the experimental geometry with a magnetic field applied along the sample surface. (b) Element-specific hysteresis loop of ferromagnetic iron film obtained by recording the intensity of the Fe  $L_3$  XMCD spectra as a function of the applied magnetic field. (c) Co  $2p$ - $3d$  XAS spectra ( $I^+$  and  $I^-$ ) and XMCD ( $I^+ - I^-$ ) spectrum of CoPc (the spectra are reported after Fe background subtraction). XMCD measurements were performed at remanence, reversing the magnetization direction for each point of the spectra. The measurements were performed at room temperature.

magnetic moment is not adequate. In a recent paper a density functional theory (DFT) analysis showed how the interaction of CoPc with the iron substrate hybridizes the  $d_{z^2}$  electrons that are lowered below the Fermi level. As a consequence the  $d$  orbitals are partially distributed at Fermi level in a spin selective way. Taking into account the van der Waals interactions at the surface the overall spin polarization is reduced.<sup>24</sup> The XMCD result is compatible with some  $d_{xz} + d_{yz}$  spin polarization revealing that the situation may be intermediate between the prediction of DFT and DFT + vdW. Different conclusions were proposed by STM analysis compared to those calculations. Here we can stress that XMCD is a high-energy probe that operates a different projection of the empty density of state on the Co site than probed by STM. XMCD results point out that magnetism is indeed a relevant aspect of the CoPc/iron system.

No XMCD was detected at the Co  $L_{2,3}$  edges for the multilayer grown on iron. In 6 ML CoPc on iron, the molecules have a molecular neighborhood, mainly characterized by molecule/molecule interaction, and resemble the free molecules which are paramagnetic. The null magnetic response of 6 ML CoPc is compatible with a paramagnetic behavior of molecules at remanence. Alternatively, it can also be explained in terms of the antiferromagnetic interactions among CoPc molecules, as observed in Ref. 43.

N atoms may have a role in the magnetic coupling between CoPc and iron. The involvement of N atoms in the magnetic coupling is predicted theoretically<sup>18</sup> and verified experimentally at the Alq/iron interface. The N magnetic moment is one-tenth of that of Co and the magnitude of XMCD at the *K* edge is much smaller than that at the *L* edge, making XMCD measurements at the N edge challenging. We do not observe an XMCD signal at the N *K* edge within our sensitivity

at room temperature, so we cannot discuss the possible role of N atoms in the coupling between molecule and substrate.

#### IV. CONCLUSIONS

In conclusion, this work demonstrates how specific molecules and ferromagnetic substrates can realize efficient spin coupling at an organic/ferromagnet hybrid interface even at room temperature. A small but finite XMCD signal is observed at the Co edge for the CoPc/Fe interface. The possible contribution of N atoms in the magnetic coupling is not detectable within our sensitivity. The onset of the magnetic coupling at the molecule/ferromagnet interface corresponds to relevant changes in the electronic properties of

CoPc molecules: (i) the strong modification of Co molecular electronic distribution upon adsorption on iron; (ii) the direct bonding between the N atoms and Fe atoms or the charge transfer between Fe and N; and (iii) the modification of C electronic structure consisting in the variation of binding-energy separation of C<sub>b</sub> and C<sub>p</sub> atoms.

#### ACKNOWLEDGMENTS

One of the authors would like to acknowledge A. Cossaro for his help in the preparation of model representation by ArgusLab. This work was carried out in the framework of the PRIN 2008 525SC7 contract coordinated by M. G. Betti.

\*annese@tasc.infm.it

<sup>1</sup>I. Zutic, J. Fabian, and S. D. Sarma, *Rev. Mod. Phys.* **76**, 323 (2004).

<sup>2</sup>Z. H. Xiong, D. Wu, Z. V. Vardeny, and J. Shi, *Nature (London)* **427**, 821 (2004).

<sup>3</sup>M. Mannini, F. Pineider, P. Saintavrit, C. Danieli, E. Otero, C. Sciancalepore, A. M. Talarico, M.-A. Arrio, A. Cornia, D. Gatteschi, and R. Sessoli, *Nat. Mater.* **8**, 194 (2009).

<sup>4</sup>H. Wende, M. Bernien, J. Luo, C. Sorg, N. Ponpandian, J. Kurde, J. Miguel, M. Piantek, X. Xu, Ph. Eckhold, W. Kuch, K. Baberschke, P. M. Panchmatia, B. Sanyal, P. M. Oppeneer, and O. Eriksson, *Nat. Mater.* **6**, 516 (2007).

<sup>5</sup>A. Scheybal, T. Ramsvik, R. Bertschinger, M. Putero, F. Nolting, and T. A. Jung, *Chem. Phys. Lett.* **411**, 214 (2005).

<sup>6</sup>P. Gambardella, S. Stepanow, A. Dmitriev, J. Honolka, F. M. F. de Groot, M. Lingenfelder, S. Sen Gupta, D. D. Sarma, P. Bencok, S. Stanesco, S. Clair, S. Pons, N. Lin, A. P. Seitsonen, H. Brune, J. V. Barth, and K. Kern, *Nat. Mater.* **8**, 189 (2009).

<sup>7</sup>S. Heutz, C. Mitra, W. Wu, A. J. Fisher, A. Kerridge, M. Stoneham, A. H. Harker, J. Gardener, H.-H. Tseng, T. S. Jones, C. Renner, and G. Aeppli, *Adv. Mater.* **19**, 3618 (2007).

<sup>8</sup>P. Gambardella, S. Rusponi, M. Veronese, S. S. Dhesi, C. Grazioli, A. Dallmeyer, I. Cabria, R. Zeller, P. H. Dederichs, K. Kern, C. Carbone, and H. Brune, *Science* **300**, 1130 (2003).

<sup>9</sup>A. R. Rocha, V. M. García-suárez, S. W. Bailey, C. J. Lambert, J. Ferrer, and S. Sanvito, *Nat. Mater.* **4**, 335 (2010).

<sup>10</sup>M. Cinchetti, K. Heimer, J.-P. Wüstenberg, O. Andreyev, M. Bauer, S. Lach, C. Ziegler, Y. Gao, and M. Aeschlimann, *Nat. Mater.* **8**, 115 (2009).

<sup>11</sup>V. A. Dediu, I. Bergenti, and C. Taliani, *Nat. Mater.* **8**, 707 (2010).

<sup>12</sup>J. Bartolomé, F. Bartolomé, L. M. García, G. Filoti, T. Gredig, C. N. Colesniuc, I. K. Schuller, and J. C. Cezar, *Phys. Rev. B* **81**, 195405 (2010).

<sup>13</sup>S. Stepanow, A. Mugarza, G. Ceballos, P. Moras, J. C. Cezar, C. Carbone, and P. Gambardella, *Phys. Rev. B* **82**, 014405 (2010).

<sup>14</sup>T. Suzuki, M. Kurahashi, and Y. Yamauchi, *J. Phys. Chem. B* **106**, 7643 (2002).

<sup>15</sup>M. Bernien, J. Miguel, C. Weis, Md. E. Ali, J. Kurde, B. Krumme, P. M. Panchmatia, B. Sanyal, M. Piantek, P. Srivastava, K. Baberschke, P. M. Oppeneer, O. Eriksson, W. Kuch, and H. Wende, *Phys. Rev. Lett.* **102**, 047202 (2009).

<sup>16</sup>K. Barberschke, *J. Phys.* **190**, 012012 (2009).

<sup>17</sup>S. Javaid, M. Bowen, S. Boukari, L. Joly, J.-B. Beaufrand, X. Chen, Y. J. Dappe, F. Scheurer, J.-P. Kappler, J. Arabski, W. Wulfhekel, M. Alouani, and E. Beaurepaire, *Phys. Rev. Lett.* **105**, 077201 (2010).

<sup>18</sup>Y. Zhan, E. Holmström, R. Lizárraga, O. Eriksson, X. Liu, F. Li, E. Carlegrim, S. Stafström, and M. Fahlman, *Adv. Mater.* **22**, 1626 (2010).

<sup>19</sup>S. R. Foster, *Chem. Rev.* **97**, 1793 (1997).

<sup>20</sup>X. Chen and M. Alouani, *Phys. Rev. B* **82**, 094443 (2010).

<sup>21</sup>A. Zhao, Q. Li, L. Chen, H. Xiang, W. Wang, S. Pan, B. Wang, X. Xiao, J. Yang, J. G. Hou, and Q. Zhu, *Science* **309**, 1542 (2005).

<sup>22</sup>S. Stepanow, P. S. Miedema, A. Mugarza, G. Ceballos, P. Moras, J. C. Cezar, C. Carbone, F. M. F. de Groot, and P. Gambardella, *Phys. Rev. B* **83**, 220401 (2011).

<sup>23</sup>C. Iacovita, M. V. Rastei, B. W. Heinrich, T. Brumme, J. Kortus, L. Limot, and J. P. Bucher, *Phys. Rev. Lett.* **101**, 116602 (2008).

<sup>24</sup>J. Brede, N. Atodiresei, S. Kuck, P. Lazić, V. Caciuc, Y. Morikawa, G. Hoffmann, S. Blügel, and R. Wiesendanger, *Phys. Rev. Lett.* **105**, 047204 (2010).

<sup>25</sup>M. T. Kief and W. F. Egelhoff, *Phys. Rev. B* **47**, 10785 (1993).

<sup>26</sup>The “search light effect” is an expression introduced in Ref. 27 to express the capability of polarized x rays to explore the electronic distribution of adsorbate molecular orbitals. According to the dipole approximation, the absorption intensity is proportional to the square of the scalar product of the electric field of the x rays and the direction of the final-state orbitals when exciting from s-like core levels. The spatial distribution of maximum (minimum) unoccupied molecular orbitals is detected by varying the relative position of the electric field vector of linearly polarized x rays and final-state orbitals, hence by rotating the sample surface with respect to the x-ray beam or by varying the polarization of the incoming light.

<sup>27</sup>J. Stöhr, *J. Electron Spectrosc. Relat. Phenom.* **75**, 253 (1995).

<sup>28</sup>G. Panaccione, I. Vobornik, J. Fujii, D. Krizmancic, E. Annese, L. Giovannelli, F. Maccherozzi, F. Salvador, A. De Luisa, D. Benedetti, A. Gruden, P. Bertoch, F. Polack, D. Cocco, G. Sostero, B. Diviacco, M. Hochstrasser, U. Maier, D. Pescia, C. H. Back, T. Greber, J. Osterwalder, M. Galaktionov, M. Sancrotti, and G. Rossi, *Rev. Sci. Instrum.* **80**, 043105 (2009).

- <sup>29</sup>I. Horcas, R. Fernández, J. M. Gómez-Rodríguez, J. Colchero, J. Gómez-Herrero, and A. M. Baro, *Rev. Sci. Instrum.* **78**, 013705 (2007).
- <sup>30</sup>H. Peisert, I. Biswas, M. Knupfer, and T. Chassé, *Phys. Status Solidi A* **206**, 2524 (2009).
- <sup>31</sup>I. Biswas, H. Peisert, M. B. Casu, B.-E. Schuster, P. Nagel, M. Merz, S. Schuppler, and T. Chassé, *Phys. Status Solidi B* **246**, 1529 (2009).
- <sup>32</sup>R. Cuadrado, J. I. Cerdá, Y. Wang, G. Xin, R. Berndt, and H. Tang, *J. Chem. Phys.* **133**, 154701 (2010).
- <sup>33</sup>E. Annese, J. Fujii, I. Vobornik, and G. Rossi, *J. Phys. Chem. C* **115**, 17409 (2011).
- <sup>34</sup>Mark A. Thompson, ArgusLab 4.0.1, Planaria Software LLC, Seattle, WA [<http://www.arguslab.com>].
- <sup>35</sup>M. M. El-Nahass, Z. El-Gohary, and H. S. Soliman, *Opt. Laser Technol.* **35**, 523 (2003).
- <sup>36</sup>N. Papageorgiou, E. Salomon, T. Angot, J.-M. Layet, L. Giovanelli, and G. Le Lay, *Prog. Surf. Sci.* **77**, 139 (2004).
- <sup>37</sup>F. Petraki, H. Peisert, I. Biswas, and T. Chassé, *J. Phys. Chem. C* **114**, 17638 (2010).
- <sup>38</sup>V. V. Maslyuk, V. Y. Aristov, O. V. Molodtsova, D. V. Vyalikh, V. M. Zhilin, Y. A. Ossipyan, T. Bredow, I. Mertig, and M. Knupfer, *Appl. Phys. A* **94**, 485 (2009).
- <sup>39</sup>R. W. Bigelow, K.-Y. Law, D. H.-K. Pan, and H.-J. Freund, *J. Electron Spectrosc. Relat. Phenom.* **46**, 1 (1988).
- <sup>40</sup>T. Kroll, V. Yu. Aristov, O. V. Molodtsova, Yu. A. Ossipyan, D. V. Vyalikh, B. Buchner, and M. Knupfer, *J. Phys. Chem. A* **113**, 8917 (2009).
- <sup>41</sup>In Ref. 22 the calculations are performed starting from a  $d^7$  configuration of a Co ion in  $D_{4h}$  crystal-field symmetry. Here, we report the correspondence between  $e_g$ ,  $b_{2g}$ ,  $a_{1g}$ , and the  $d$  orbitals within this theoretical framework:  $e_g \rightarrow (d_{yz}, d_{zx})$ ,  $b_{2g} \rightarrow (d_{xy})$ ,  $a_{1g} \rightarrow d_{3z^2-y^2}$ .
- <sup>42</sup>H. Ebert, V. Popescu, D. Ahlers, G. Schütz, L. Lemke, H. Wende, P. Srivastava, and K. Baberschke, *Europhys. Lett.* **42**, 295 (1998).
- <sup>43</sup>X. Chen, Y.-S. Fu, S.-H. Ji, T. Zhang, P. Cheng, X.-C. Ma, X.-L. Zou, W.-H. Duan, J.-F. Jia, and Q.-K. Xue, *Phys. Rev. Lett.* **101**, 197208 (2008).